Supporting information

para-Xylene selective Metal-Organic Frameworks: a case of topology-directed selectivity

Frederik Vermoortele, Michael Maes, Peyman Z. Moghadam, Matthew J. Lennox, Florence Ragon, Mohammed Boulhout, Shyam Biswas, Katrien G. M. Laurier, Isabelle Beurroies, Renaud Denoyel, Maarten Roeffaers, Norbert Stock, Tina Düren, Christian Serre, Dirk E. De Vos

Table of contents

Visualization of pore space	S2
Simulated single compound isotherms	S2
Information about loading and interaction energies	S3
Integral adsorption enthalpy	S4
Pulse chromatographic experiments	S5
Breakthrough experiment	S6
Comparison with KBaY zeolite	S7
MOF synthesis and characterization	S8
MOF stability	S14
Experimental procedures	S15
Computational details	S16

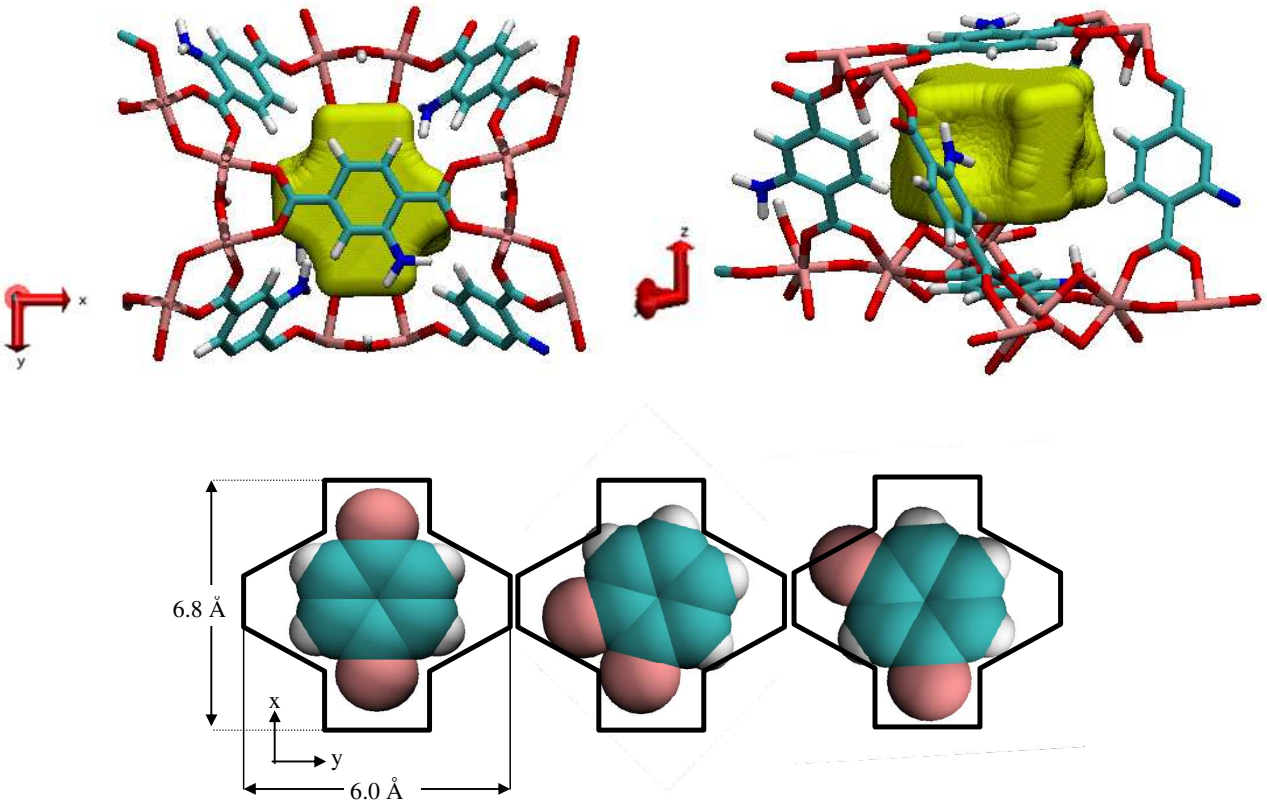

Figure S1. Illustration of the complex pore space (yellow[S1]) in the small tetrahedral pores (top). Schematic illustration of how pX fits easily into the cross-shaped pore space while there is some overlap for oX. mX does not fit into the pore space at all.

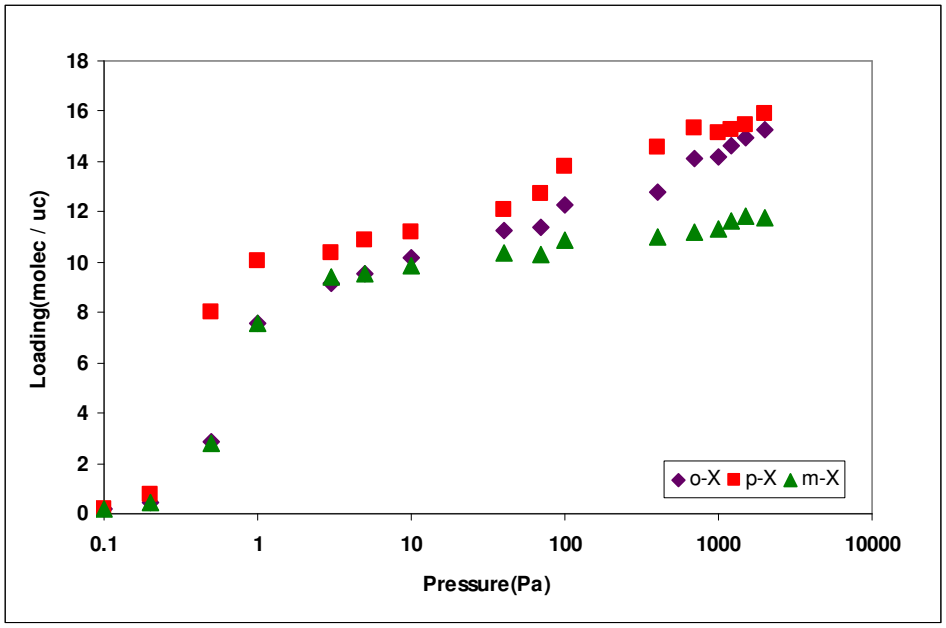

Figure S2. Simulated single component isotherms of pX, oX and mX in MIL-125(Ti)-NH_2 at 300 K.

Table S1. Adsorbate-framework potential energies for xylene molecules in the octahedral and tetrahedral cages of MIL-125 (Ti)-NH_2 calculated from NVT Monte Carlo simulations at 300 K. A single molecule was loaded into the octahedral and tetrahedral cages, respectively. Note that mX does not fit into the small tetrahedral pores.

	Large octahedral cages	**Small tetrahedral cages**
	U (kJ/mol)	**U (kJ/mol)**
pX	-52.57	-51.44
oX	-48.45	-44.41

Table S2. Interaction energies for equimolar xylene mixtures at 1 kPa and 300 K in MIL-125(Ti)-NH_2.

	Potential energy (kJ/mol)			
	pX	**oX**	**pX**	**mX**
adsorbate-adsorbate	-18.84	-12.14	-18.95	-11.65
adsorbate-framework	-51.75	-48.3	-51.7	-48.32

Table S3. Breakdown of the loadings into the octahedral and tetrahedral cages of MIL-125(Ti)-NH_2 for equimolar xylene mixtures at 1 kPa and 300 K

Mixture	**Large octahedral cages**	**Small tetrahedral cages**	**Total**
	N (molec / uc)	**N (molec / uc)**	**N (molec / uc)**
pX	8	3.4	11.4
oX	3.6	0.4	4
pX	8.2	3.7	11.9
mX	3.5	0	3.5

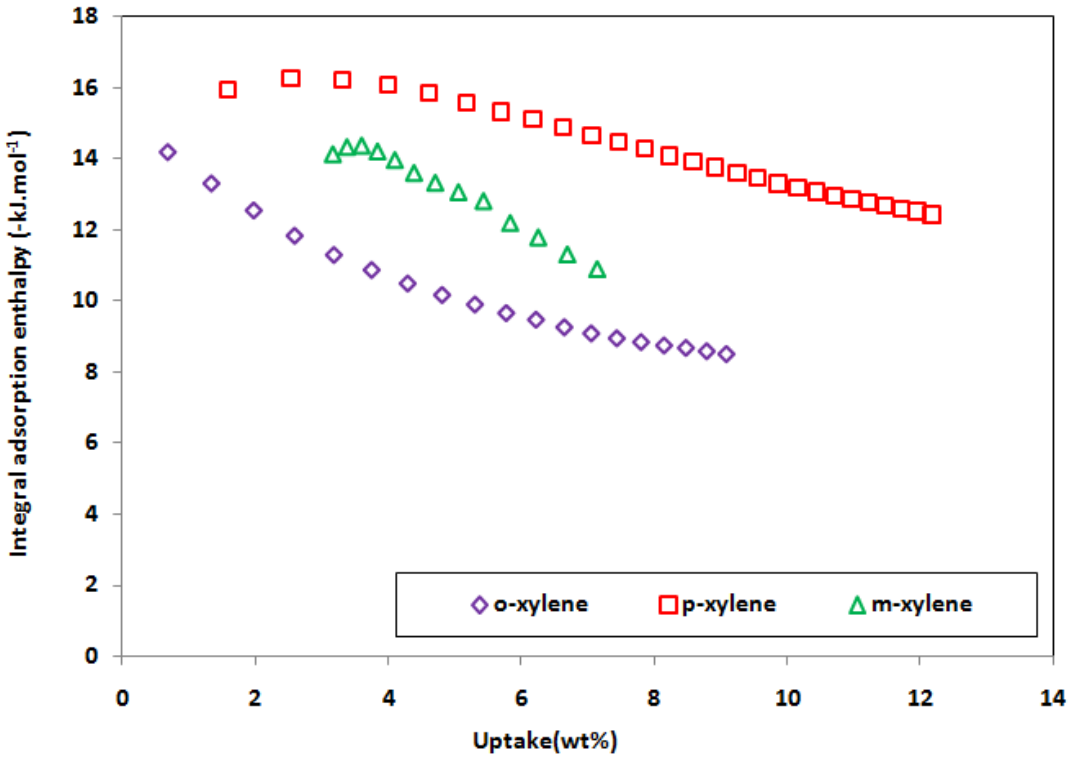

Figure S3. Integral adsorption enthalpy ΔH (kJ.mol^{-1}) of xylene isomers on MIL-125(Ti)-NH_2 as a function of uptake (wt%).

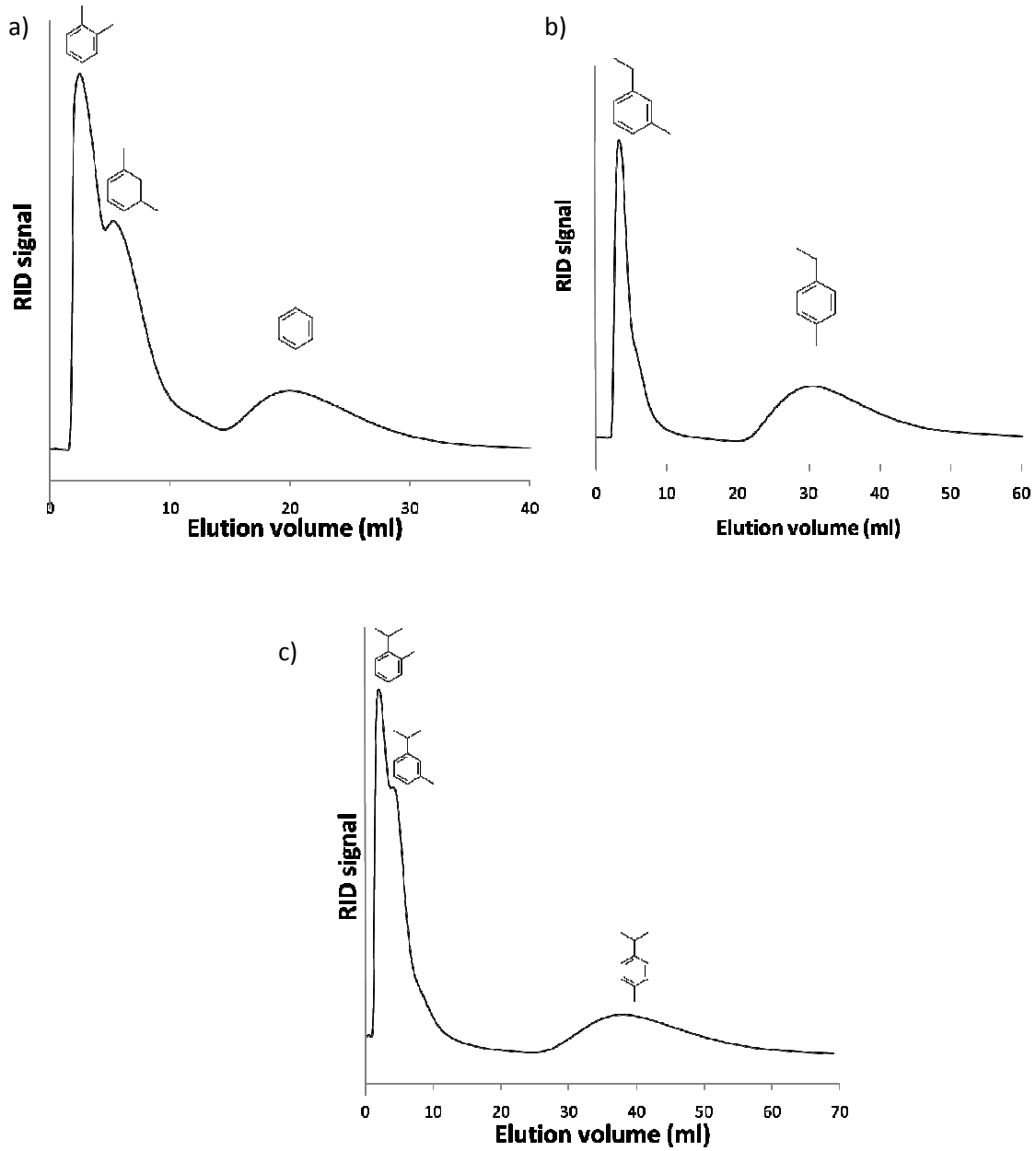

Figure S4. Chromatographic separation of a mixture of (a) xylene isomers, (b) ethyltoluene isomers and (c) cymene isomers on a column packed with MIL-125(Ti)-NH_2 crystallites and with heptane as the desorbent at 298 K. The signal intensity of the refractive index detector (RID) is shown versus the eluted volume. The curves have been corrected for the dead volume of the column.

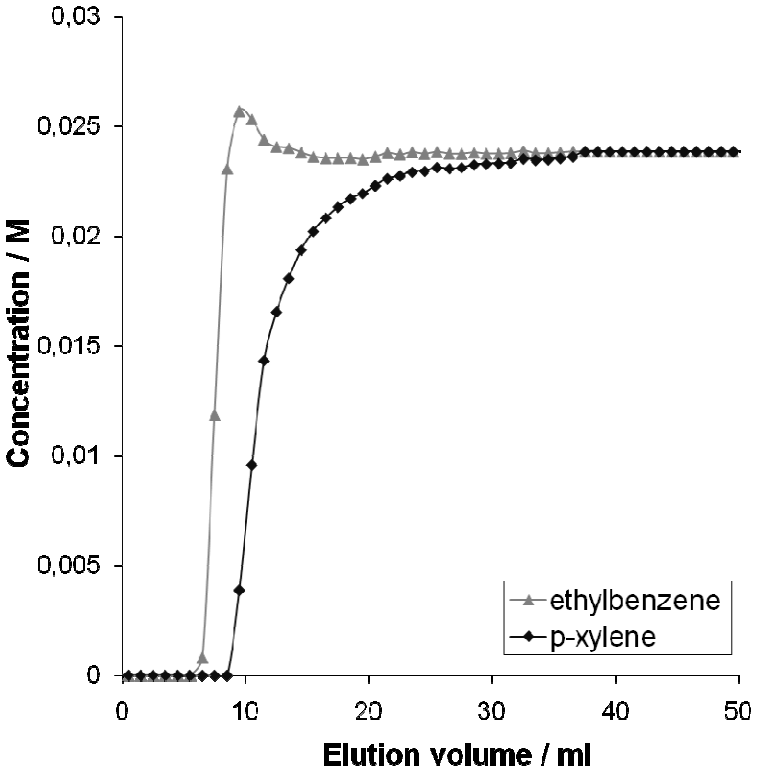

Figure S5. Breakthrough profile for a binary solution of ethylbenzene and *p*-xylene in heptane (inlet concentrations 0.024 M) on a column filled with MIL-125(Ti)-NH_2 crystallites at 298 K: effluent concentration (M) as a function of the eluted volume (ml). The curve has been corrected for dead volume.

Comparison with classical adsorbents

For comparison, competitive batch adsorption experiments have been performed on zeolites KBaY and ZSM-5 at 0.35 M (the concentration at which maximal uptake is observed in Figure 4) (Table S4).

Table S4. Uptake (wt. %) from an equimolar, 0.35 M mixture of pX and mX on MIL-125(Ti)-NH_2, zeolite KBaY and ZSM-5. Separation factors $\alpha_{pX/mX}$ are shown in the last row.

	MIL-125(Ti)-NH_2	**KBaY**
pX uptake at 0.35 M (wt%)	12	15
mX uptake at 0.35 M (wt%)	4	3.2
Selectivity ($\alpha_{pX/mX}$)	3.1	4

The *para-/meta*-xylene separation on MIL-125(Ti)-NH_2 was compared to the one obtained on zeolite KBaY, a zeolite with FAU-topology that is used for this application on an industrial scale. In zeolites with the FAU-topology, the selectivity, unlike on ZSM-5 or silicalite, arises from efficient molecular packing of the para-xylene molecules in the framework (A. Méthivier in *Zeolites for Cleaner Technologies, Catalytic Science Series - Vol. 3* (Eds.: M. Guisnet, J. P. Gilson), Imperial College Press, London, **2002**, pp. 209–221). Molecular packing is also found to be the key selectivity determining mechanism in the octahedral cages of MIL-125(Ti)-NH_2.

When comparing MIL-125(Ti)-NH_2 with zeolite KBaY, it is clear that MIL-125(Ti)-NH_2 can withstand the comparison with zeolite KBaY. Both materials appear to have similar uptake capacities and separation factors, underlining the potential of MOF structures with this specific topology for xylene separation.

MOF synthesis and characterization

MIL-125(Ti)-NH_2 was synthesized by dissolving 7.5 g 2-aminoterephthalic acid (Alfa Aesar, 99%) in 100 mL of *N*,*N*-dimethylformamide (DMF) (Carlo Erba, pure) and 25 mL of methanol (MeOH) (Prolabo, 99.9%) at room temperature under stirring. 7.5 mL of Ti(O*i*Pr)$_4$ (Acros organics, 98+ %) was added at the end. The mixture was placed in a 475 mL Teflon liner and then inserted into a metallic Parr digestion bomb at 150 °C during 16 hours. At room temperature, the yellow solid was recovered by filtration, washed with acetone and dried under air at room temperature. In order to remove free acid which can remain in the pores, the as-synthesized product was dispersed at room temperature in DMF and stirred overnight. In order to remove the DMF out of the pores, the same procedure was repeated twice using MeOH instead of DMF. The final product was dried in the oven at 100°C overnight.

MIL-125(Ti) was synthesized by following the synthesis conditions reported previously[7a] and was activated using the same procedure as used for MIL-125(Ti)-NH_2.

CAU-1(Al)-NH_2 was synthesized by microwave-assisted heating. A mixture of $AlCl_3 \cdot 6H_2O$ (232 mg, 0.13 mmol) and H_2BDC-NH_2 (58 mg, 0.32 mmol) in methanol (3.2 mL) was placed in a Pyrex sample tube. The tube was sealed and placed in a microwave synthesizer (Biotage). The resulting mixture was heated at 145 °C for 3 min under stirring (300 r/s). After cooling, the yellow powder was collected by centrifugation, washed thoroughly with water and dried in an oven at 150 °C under air for 12 hours. The yield was 40 mg (0.05 mmol, 21% based on Al-salt).

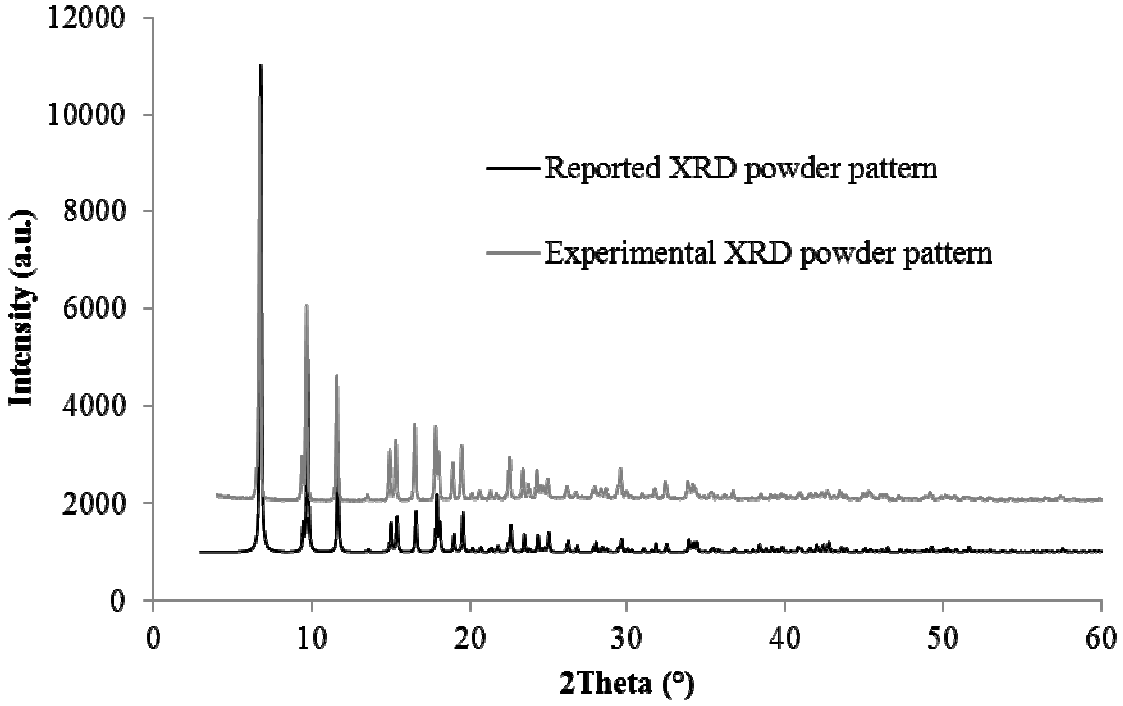

Figure S6. Experimental XRD powder pattern of the activated MIL-125(Ti)-NH_2 product (grey) compared with the reported XRD powder pattern of the non-modified MIL-125(Ti) phase (black).[7a]

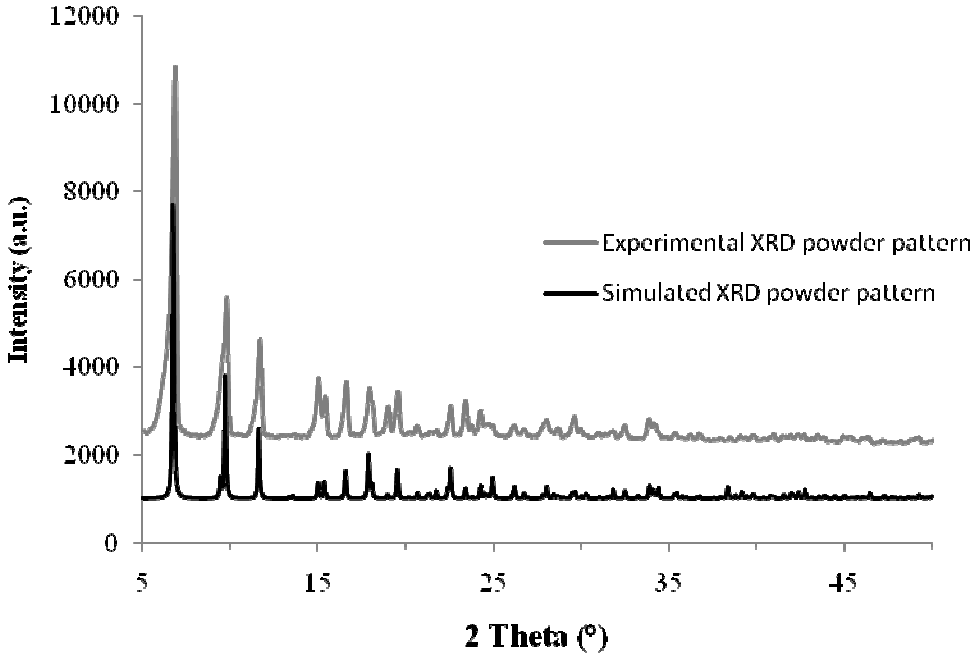

Figure S7. Experimental XRD powder pattern of the activated MIL-125(Ti) product (grey) compared with the reported XRD powder pattern of MIL-125(Ti) (black).[7a]

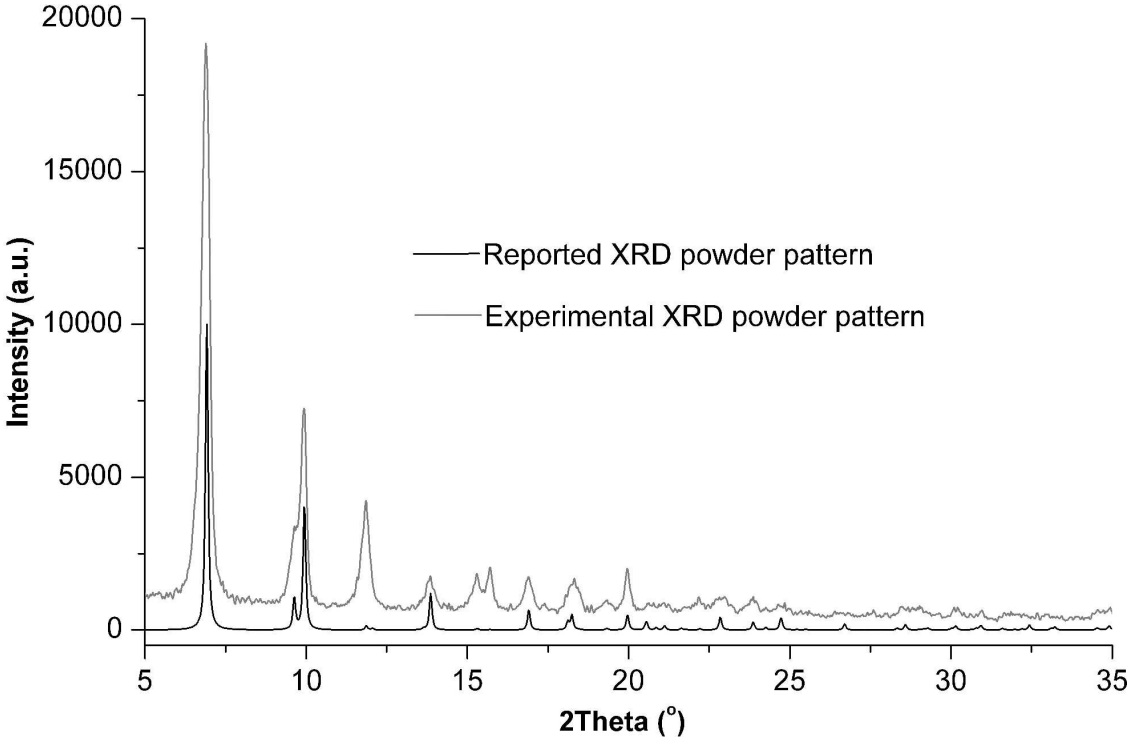

Figure S8. Experimental XRD powder pattern of the activated CAU-1-NH_2 product (grey) compared with the reported XRD powder pattern of the CAU-1-$NH(CH_3)$ phase (black).[7c]

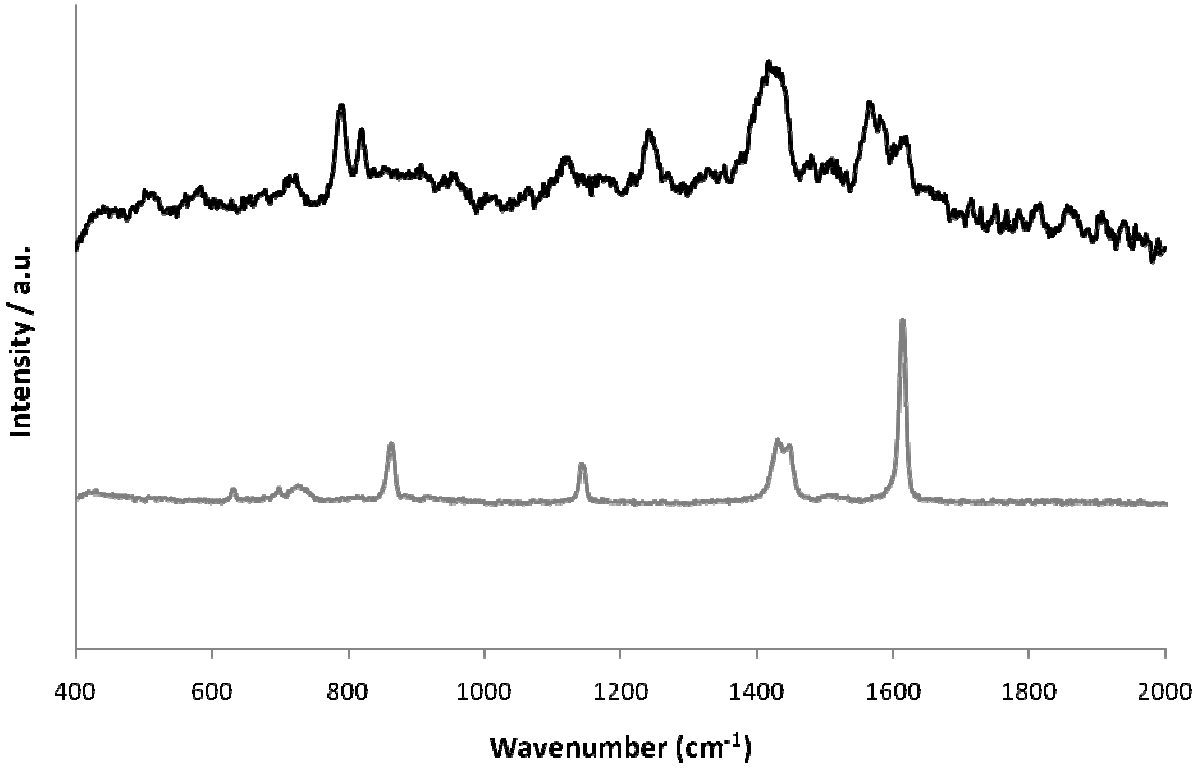

Figure S9. Raman spectrum of MIL-125(Ti)-NH_2 (black) and MIL-125(Ti) (grey).

The figure above compares the Raman spectra of MIL-125(Ti)-NH_2 and MIL-125(Ti). The most intense peaks are at ~ 797 cm^{-1}, 828 cm^{-1}, 1255 cm^{-1}, 1418 cm^{-1}, 1583 cm^{-1} and 1626 cm^{-1} for MIL-125(Ti)-NH_2 and 863 cm^{-1}, 1141 cm^{-1}, 1430 cm^{-1}, 1447 cm^{-1} and 1613 cm^{-1}. As these shifts are different from the typical anatase (399 cm^{-1}, 515 cm^{-1}, 519 cm^{-1} and 639 cm^{-1})[S2] and rutile (447 cm^{-1}, 612 cm^{-1} and 826 cm^{-1})[S3] Raman shifts, there is no indication of any residual TiO_2 in the materials.

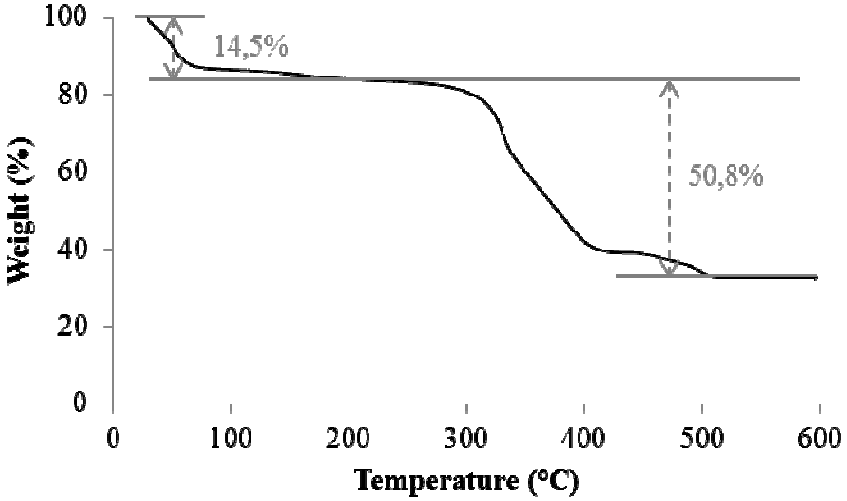

Figure S10. TGA of activated MIL-125(Ti)-NH_2 product under O_2 (heating rate of 2°C per minute) (8 mg of solid).

Two weight loss steps were observed on the TGA curve: first the departure of the guest molecules (H_2O, MeOH and DMF) in the range 25-250°C (14.5 %); the second step is due to the decomposition of the framework to produce TiO_2 anatase and is associated with the departure of the organic linker (experimental: 51%; calculated: 50.9%).

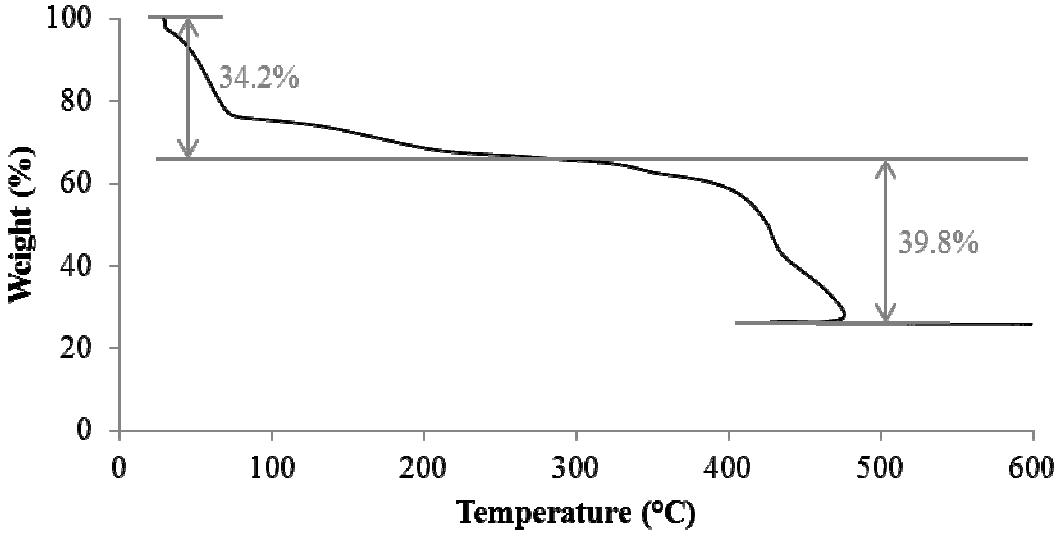

Figure S11. TGA of activated MIL-125(Ti) product under O_2 (heating rate of 2°C per minute) (5 mg of solid).

Two weight-loss steps were observed on the TGA curve: a first one, corresponding to the departure of the guest molecules (H_2O, MeOH and DMF) in the range 25-300°C (34.2%); the second one is due to the decomposition of the framework to produce TiO_2 anatase and is associated with the combustion of the organic linker (experimental: 39.8%; calculated: 38.8%).

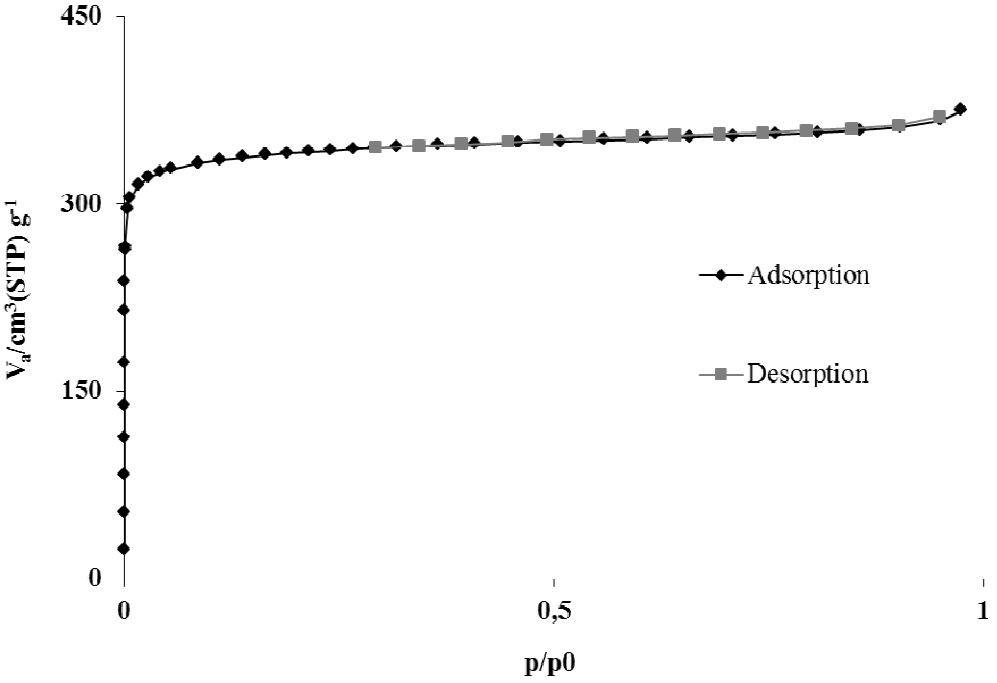

Figure S12. Nitrogen adsorption isotherm of MIL-125(Ti)-NH_2 at T = 77K (p_0 = 1 bar).

Nitrogen physisorption at 77 K has been performed on the material after a treatment under primary vacuum at 150°C overnight. A BET specific surface area of 1380 $m^2.g^{-1}$ is obtained.

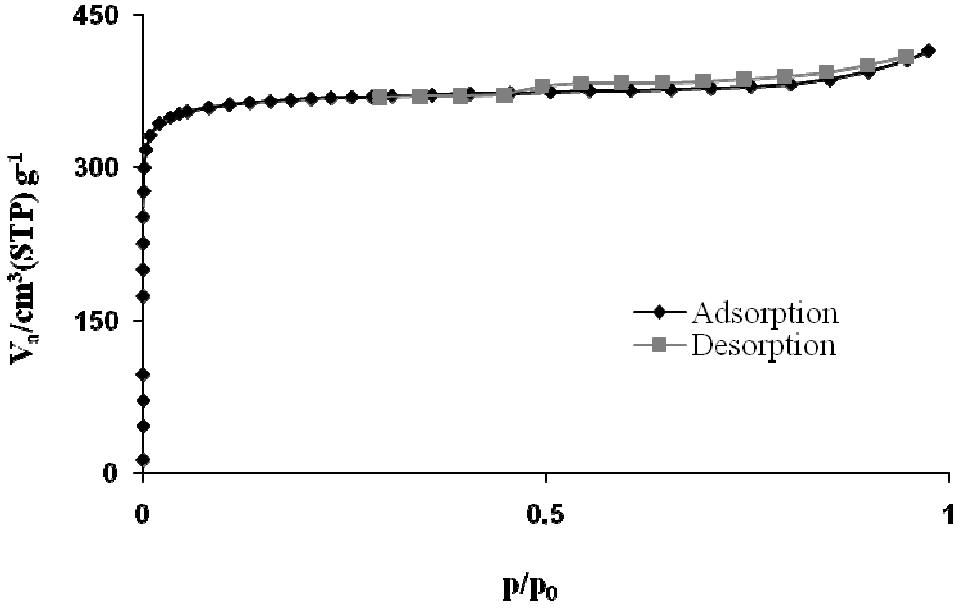

Figure S13. Nitrogen adsorption isotherm of MIL-125(Ti) at T = 77K (p_0 = 1 bar).

Nitrogen physisorption at 77 K has been performed on MIL-125(Ti) after a treatment under primary vacuum at 175°C overnight. A BET specific surface area of 1446 $m^2.g^{-1}$ is obtained.

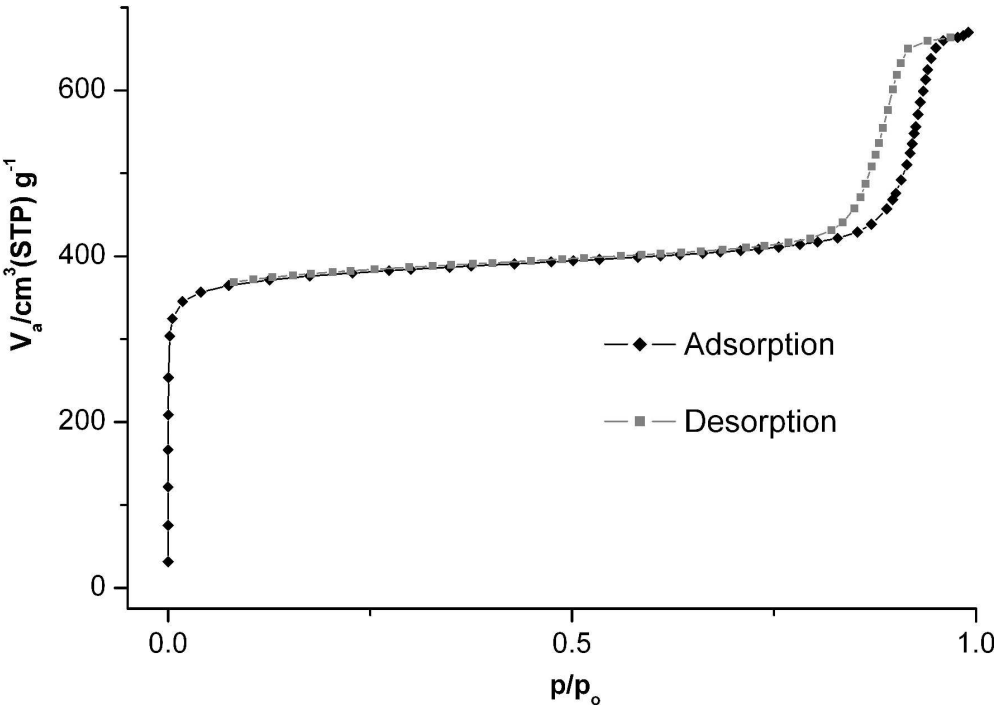

Figure S14. Nitrogen adsorption-desorption isotherms of CAU-1(Al)-NH_2 at T = 77K (p_0 = 1 bar).

Nitrogen physisorption at 77 K has been performed on CAU-1(Al)-NH_2 after a treatment under primary vacuum at 150 °C for 12 hours. A BET specific surface area of 1495 $m^2.g^{-1}$ is obtained.

MOF stability in xylene separation

All of the structures have proven to be stable under the conditions tested. For MIL-125(Ti)-NH_2, adsorption of xylenes on a column of the material has been repeated over 15 times. After each cycle the column was regenerated using pure heptane. The retention volume, indicative for the capacity, and the separation factor did not differ between the first and the last cycle. Furthermore, the material in the column was analysed using XRD measurements. As can be seen from Figure S15, the XRD pattern is identical to that of activated freshly synthesized MIL-125(Ti)-NH_2.

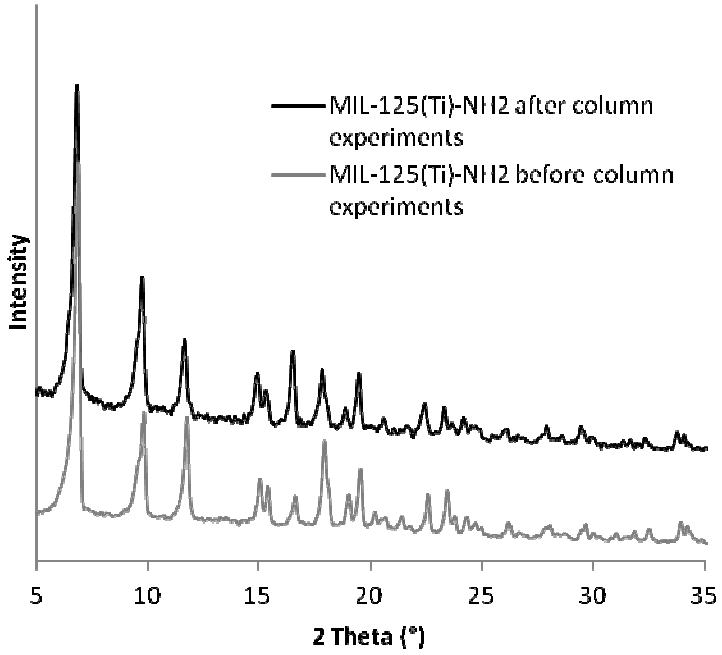

Figure S15. Experimental XRD powder pattern of the freshly synthesized activated MIL-125(Ti)-NH_2 (before column experiments) and the pattern of the same sample after exposure to column conditions for over 15 cycles.

The stability of MIL-125(Ti) and CAU-1(Al)-NH_2 can be assessed by comparing adsorption data for a sample used within a couple of days after synthesis, with data obtained from the same sample after it has been stored under ambient conditions for over three months. As can be seen from Table S5, there is no difference in uptake.

Table S5. Maximum uptake capacity of pX (wt%) out of heptane on CAU-1(Al)-NH_2, MIL-125(Ti) and MIL-125(Ti)-NH_2. Separation factors $\alpha_{pX/mX}$ are shown in the bottom row.

	CAU-1(Al)-NH_2	**MIL-125(Ti)**	**MIL-125(Ti)-NH_2**
initial max. capacity pX at 0.4 M (wt%)	9	8.4	14.3
max. capacity pX after 3 months at 0.4M (wt%)	8.9	8.4	14.1

Experimental procedures

Liquid phase adsorption

Liquid phase batch adsorption experiments were carried out at 298 K in 1.8 ml glass vials filled with 0.025 g of adsorbent and a solution of aromatics in heptane following a literature procedure[5a]. Uptakes were directly calculated from GC output data. For competitive adsorption experiments, equimolar mixtures of C_8-alkylaromatics were used. Separation factors α_{ij} were calculated using formula (1):

$$\alpha_{ij} = \left(\frac{q_i}{q_j}\right) \times \left(\frac{c_j}{c_i}\right) \quad (1)$$

with q_i and q_j the amount (mol g^{-1}) of compounds *i* and *j* adsorbed per g of MOF, and c_i and c_j the concentrations (mol L^{-1}) of compounds *i* and *j* remaining in the external liquid phase.

Pulse and breakthrough chromatographic experiments were performed following a literature procedure[5a]. Columns were hand made by loading approximately 0.6 g of adsorbent into a stainless steel column (*L* = 5 cm, *D* = 0.45 cm) under nitrogen atmosphere. The column was further activated by flushing with nitrogen at 150°C overnight.

For breakthrough experiments an equimolar mixture of C_8-alkylaromatics is used and average selectivities were calculated using eqn (1). For each compound, the adsorbed amounts *q* were calculated by integration of the curves using eqn (2):

$$q = \int_0^t u \times (C_{in} - C_{out}) dt \quad (2)$$

with C_{in} and C_{out} the concentrations (mol L^{-1}) of the adsorbate in the liquid feed and eluent and *u* the volumetric flow rate of the feed (L min^{-1}), respectively. As the column is fed with an equimolar mixture, the average separation factor α can be written as $\alpha_{ij} = q_i / q_j$, where q_i is the amount adsorbed of the secondly eluting compound, and q_j the amount adsorbed of the first eluting compound. Regeneration of the column is performed by flushing with typically 100 ml of pure solvent at 60°C.

Pulse chromatographic experiments have been performed at room temperature using a HPLC column filled with adsorbent. The separation factor is then calculated according to eqn (3):

$$\alpha_{ij} = \frac{(\mu_i - \mu_{tc})}{(\mu_j - \mu_{tc})} \quad (3)$$

with μ_i the first moment of the secondly eluting compound, μ_j the first moment of the firstly eluting compound and μ_{tc} the first moment of 1,3,5-triisopropylbenzene, a tracer compound which is too large to enter the pores and thus is indicative for the dead volume. First moments are calculated using ChemStation software from Agilent.

Microcalorimetry

In each experiment, 0.025 g sample was placed in a stainless steel container and activated (thermal treatment at 150°C for 16 hours). After the activation, the MOF is weighed and 800 µL of solvent (heptane) is added to the reaction vessel through the septum. The dispersion is stirred in the container. Then the titration container is loaded into the TAM III calorimeter (TA instruments). The container must be equilibrated in the calorimeter at 25 °C before initiation of the experiment. Note that in the reference side, a container is placed loaded with only the same quantity of solvent as in the sample side. The heat flow mode of the apparatus is used during the experiment. In the Isothermal Titration Calorimetry (ITC), the liquid titrant (adsorbate) can be added to the reaction container using a motor driven syringe pump through a fine cannula. A total volume of 200 µl is added step by step (generally 20 injections of 10 µL). Between two successive injections the equilibrium must be reached. In this experiment, the heat flow versus time is measured for each injection. From these data, the integrated heat is calculated. The measured heat ($Q_{measured} = Q_{displacement} + Q_{dilution}$) corresponds to the adsorption and the dilution phenomena. In order to subtract the heat change associated with the dilution, an experiment without the sample (dilution of the adsorbate) is performed by using the same conditions. For each injection, the corresponding equilibrium concentration is determined from the adsorption isotherms.

Computational details

Details of the computational screening

For a total of 25 MOFs, we calculated the pore size distributions using the method by Gelb and Gubbins.[S4] This method gives the pore size as the largest sphere that does not overlap with any of the framework atoms. If the kinetic diameter (pX: 5.8 Å, oX: 6.4 Å, mX: 6.5 Å) is responsible for molecular sieving, MOFs with pore size between 5.8 and 6.4 Å should be selective for pX. However, the picture is more complicated and it is actually the shape of the non-spherical xylene molecules that can be responsible for molecular sieving (compare Figure S1). Therefore, we expanded the range of pore sizes looking at nine MOFs with pore sizes between 4 and 7 Å in more detail by simulating the selectivities of equimolar xylene mixtures at 1 kPa and 300 K to identify MOFs that are pX selective such as MIL-125(Ti)-NH_2.

Molecular simulation details

The adsorption isotherms of the xylene molecules in MIL-125(Ti)-NH_2 were obtained from grand canonical Monte Carlo (GCMC)[S5] simulations carried out using the MuSiC simulation code[S6]. Monte Carlo moves included insertion, deletion, translation, rotation and, in the case of binary mixtures, identity swap and re-insertion moves to achieve faster equilibration times. Our simulation cell consisted of 8 (2×2×2) unit cells in which each unit cell (18.6540 Å ×18.6540 Å ×18.1440 Å) consisted of 272 atoms. We considered the MOF as rigid and the framework atoms were kept fixed at their crystallographic positions. Our GCMC simulations mimicked vapor phase adsorption (i.e. in contrast to the experiments, no solvent was considered) and the input fugacities were calculated from the Peng-Robinson equation of state. For the calculation of both the fluid-fluid and the fluid-framework interactions, the Lennard-Jones potential was used with a cut-off radius of 15 Å. The Lennard Jones parameters for all the framework were taken from the Dreiding force field[S7] except for titanium which was taken from the UFF force field.[S8] The OPLS force field was used to model the xylene isomers. In this model, all atoms are defined explicitly except for the CH_3 groups which were modelled as united atoms i.e. as a single sphere.[S9] The Lorentz-Berthelot mixing rules were used to calculate mixed Lennard Jones parameters. The Ewald summation technique[S10] was used to calculate the interactions between the guest and the framework, while guest-guest electrostatic interactions were calculated using the technique described by Wolf *et al*.[S11]

Supporting information references:

(S1) L. Sarkisov and A. Harrison "Computational structure characterization tools in application to ordered and disordered porous materials", *Molecular Simulation*, accepted

(S2) Chen X., Liu L., Yu P. Y. and Mao S. S., *Science*, **2011**, *331*, 746-750.

(S3) A. Swamy and B. C. Muddle, *Appl.phys.lett*., **2006**, 163118.

(S4) Gelb, L. D. and K. E. Gubbins (1999). "Pore size distributions in porous glasses: A computer simulation study." Langmuir 15(2): 305-308.

(S5) Frenkel, D.; Smit, B., *Understanding of Molecular Simulation: from Algorithms to Applications*. 2nd ed.; Academic Press: San Diego, 2002.

(S6) Gupta, A.; Chempath, S.; Sanborn, M. J.; Clark, L. A.; Snurr, R. Q., Object-Oriented Programming Paradigms for Molecular Modeling, *Mol. Simul.,* **2003**, *29***,** 29.

(S7) Mayo, S. L.; Olafson, B. D.; Goddard, W. A., Dreiding - a Generic Force-Field for Molecular Simulations. *J. Phys. Chem.,* **1990**, *94*, 8897-8909.

(S8) Rappe, A. K.; Casewit, C. J.; Colwell, K. S.; Goddard, W. A.; Skiff, W. M., Uff, a Full Periodic-Table Force-Field for Molecular Mechanics and Molecular-Dynamics Simulations. *J. Am. Chem. Soc.,* **1992,** *114*, 10024-10035.

(S9) Jorgensen, W. L.; Nguyen, T. B. *Journal of Computational Chemistry*, **1993**, *14*, 195-205.

(S10) Dufner, H.; Kast. S.M.; Brickmann, J.; Schlenkrich, M., Ewald, Summation Versus Direct Summation of Shifted-Force Potentials for the Calculation of Electrostatic Interactions in Solids: A Quantitative Study, *Journal of Computational Chemistry*, **1997**, *18*, 660-676.

(S11) Wolf, D.; Keblinski, P.; Phillpot, S. R.; Eggebrecht, J., *J. Chem. Phys.*, **1999**, *110*, 8258-8282.